Influence of storage and buffer composition on the mechanical behavior of flowing red blood cells

Adlan Merlo, Sylvain Losserand, François Yaya, Philippe Connes, Magalie Faivre, Sylvie Lorthois, Christophe Minetti, Elie Nader, Thomas Podgorski, Céline Renoux, et al.

Manuscript submitted to **Biophysical***Journal*
Article

Influence of storage and buffer composition on the mechanical behavior of flowing red blood cells

Adlan Merlo[1,2,3], Sylvain Losserand[1,4], François Yaya[1,4], Philippe Connes[1,5,6], Magalie Faivre[1,7], Sylvie Lorthois[1,2], Christophe Minetti[8], Elie Nader[1,5,6], Thomas Podgorski[1,4,9], Céline Renoux[1,5,6,10], Gwennou Coupier[1,4,*], and Emilie Franceschini[1,11,**]

[1]GDR MECABIO, France
[2]Institut de Mécanique des Fluides de Toulouse (IMFT), Université de Toulouse, CNRS, Toulouse, France
[3]Biomechanics and Bioengineering Laboratory (UMR 7338), Université de Technologie de Compiègne - CNRS, 60203 Compiègne, France
[4]Université Grenoble Alpes, CNRS, LIPhy, F-38000 Grenoble, France
[5]Team 'Vascular Biology and Red Blood Cell', Laboratoire Interuniversitaire de Biologie de la Motricité (LIBM) EA7424, Université Claude Bernard Lyon 1, Université de Lyon, Villeurbanne, France
[6]Laboratoire d'Excellence du Globule Rouge (Labex GR-Ex), PRES Sorbonne, Paris, France
[7]Univ Lyon, CNRS, INSA Lyon, Ecole Centrale de Lyon, Université Claude Bernard Lyon 1, CPE Lyon, INL, UMR5270, 69622 Villeurbanne, France
[8]Aero Thermo Mechanics CP 165/43, Université libre de Bruxelles, 50, avenue Frankin-Roosevelt, CP16/62, B-1050 Brussels, Belgium
[9]Université Grenoble Alpes, CNRS, Grenoble INP, LRP, F-38000 Grenoble, France
[10]Service de biochimie et biologie moléculaire, Hospices Civils de Lyon, Lyon, France
[11]Aix-Marseille Univ, CNRS, Centrale Marseille, LMA, Turing Center for Living Systems, Marseille, France
[*]Correspondence: gwennou.coupier@univ-grenoble-alpes.fr
[**]Correspondence: franceschini@lma.cnrs-mrs.fr

ABSTRACT

On-chip study of blood flow has emerged as a powerful tool to assess the contribution of each component of blood to its overall function. Blood has indeed many functions, from gas and nutrient transport to immune response and thermal regulation. Red blood cells play a central role therein, in particular through their specific mechanical properties, that directly influence pressure regulation, oxygen perfusion, or platelet and white cells segregation towards endothelial walls. As the bloom of in-vitro studies has led to the apparition of various storage and sample preparation protocols, we address the question of the robustness of the results involving cell mechanical behavior against this diversity. The effects of three conservation media (EDTA, citrate and glucose-albumin-sodium-phosphate) and storage time on the red blood cell mechanical behavior are assessed under different flow conditions: cell deformability by ektacytometry, shape recovery of cells flowing out of a microfluidic constriction, and cell flipping dynamics under shear flow. The impact of buffer solutions (phosphate-buffered saline and density-matched suspension using iodixanol/Optiprep) are also studied by investigating individual cell flipping dynamics, relative viscosity of cell suspensions and cell structuration under Poiseuille flow. Our results reveal that storing blood samples up to seven days after withdrawal and suspending them in adequate density-matched buffer solutions has in most experiments a moderate effect on the overall mechanical response, with a possible rapid evolution in the first three days after sample collection.

SIGNIFICANCE

Blood is in intimate contact with all organs in the body, supplying oxygen, nutrients and drugs while removing waste. It carries cells involved in immune response, wound repair and tumor dissemination. Blood is easily collected, revealing the presence of disease through biomarker analysis. It is storable and transfusable. Thus, blood is the subject of many in-vitro studies for research and medical purposes. Guidelines associated to sample preparation or storage conditions have been established, but these may affect its mechanical behavior. In this collaborative study, we provide new guidelines to minimize the impact of specific experimental requirements (e.g. density matching, blood freshness) by focusing on the single or collective motion of red blood cells in a large range of flow conditions.

INTRODUCTION

In human blood, the volume fraction of red blood cells (RBCs), also called haematocrit, is usually between 35 and 50% while other cells, platelets and white blood cells, occupy less than 1% of blood volume. RBCs are therefore considered as the main contributors to the rheological properties of blood.

At the macroscopic scale i.e. in large vessels or in shear rheometry, blood behaves roughly like a Newtonian fluid with a viscosity of about 3-4 mPa.s at high shear rates (above 10^3 s^{-1}) (1). At lower shear rates, however, it exhibits a strong shear-thinning behavior that is related to both aggregation and deformability of RBCs (2, 3): viscosity can reach values of order 100 mPa.s at shear rates around 0.1 s^{-1} (2). In a frequency range that is relevant to blood circulation, viscoelastic properties can emerge as a consequence of RBC elasticity (4).

In small vessels, a cell-free layer, containing only plasma, near the vessels walls was first observed by Poiseuille (5), leading to a centered distribution of RBCs in the vessel cross section. This flow structure induces a decrease of the apparent viscosity with vessels diameters (Fåhræus-Lindquist effect (6)) until a critical diameter is reached and under which the effect is reversed. It also induces a decrease of the haematocrit in these small vessels compared to larger ones (Fåhræus effect (7, 8)). Hydrodynamic interactions between cells and with the walls are at the origin of these phenomena (9–16). They are themselves strongly influenced by the mechanical properties of the RBCs. The centered RBC distribution also influences their repartition at the level of bifurcations, leading to a heterogeneous distribution of the haematocrit in the microcirculation (17–25).

The presence of proteins in plasma, especially fibrinogen, is responsible for the formation of RBC aggregates at low shear rates that are often shaped like stacks of coins (*rouleaux*) due to the flat shape of RBCs, or more irregular depending on flow conditions. RBC aggregation is the main cause of blood shear thinning (2) and is also responsible for a weak yield stress (26). While the exact contribution of the two main mechanisms of aggregation (depletion (27) or bridging (28, 29)) is still debated, experimental and theoretical investigations have shown that the morphology and stability of aggregates are strongly influenced by mechanical parameters of the RBC membrane, such as bending modulus and shear modulus (30–32). Decreased RBC deformability has been found to be associated with lower RBC aggregation but increased RBC aggregates robustness (33, 34).

The RBC membrane is made of a phospholipid bilayer including different types of trans-membrane proteins (Band 3 ion channels, glycophorins...), whose main properties are a strong area dilation modulus of about 400 mN/m (quasi-inextensible membrane), a bending modulus of about 10^{-19} J and a shear viscosity of about 0.7 μN.s/m (35). The internal side of the membrane is covered with a cytoskeleton made of a dense network of spectrin filaments that is connected to trans-membrane proteins via anchoring proteins. The cytoskeleton maintains the structural integrity of the membrane and conveys shear elasticity with a modulus in the 5-10 μN/m range (35). Many works have demonstrated that there may be a link between RBC metabolism and its deformability and some authors suggest that remodelling of the spectrin network and its links with the membrane may occur as an active, ATP consuming process (36). RBCs also maintain their shape by regulating the osmotic exchange through their membrane thanks to ion channels. Channellopathies are a group of diseases where ion and water exchanges are impaired leading to RBC shape and deformability alterations (37–40). The intimate relationship between RBC structure, metabolism, regulation and mechanical properties suggests that the quality and composition of the suspension medium (plasma or buffer) may have an impact on RBC deformability, shape and behavior in flow.

After a first set of pioneering studies in the second part of the 20^{th} century (9, 17, 41–45), the emergence of microfluidic techniques has led to a burst of research dedicated to RBC dynamics in flow, in particular regarding microcirculation issues. *In vitro* studies of blood flow allow to control separately the parameters implied in the phenomena, which are quite numerous even if one focuses only on the mechanical aspects of the problem, *i.e.* leaving biological considerations apart (*e.g.* interactions with platelets and white cells, adhesion phenomena...). This also allows for more quantitative imaging and therefore quantification of cell shape, dynamics, concentration or velocities in a controlled flow environment. Due to the variability of plasma composition between subjects, its time dependence for a given subject and the need to control or suppress parameters such as RBC aggregation, most authors use buffers of controlled composition to re-suspend blood cells at a chosen haematocrit after separating them from plasma.

Sedimentation of RBCs is also a crucial point regarding in-vitro experiments. In plasma, isolated cells sediment at velocities of order the micron/s (46). Aggregates of cells sediment even faster. These velocities are sufficient to modify deeply the distribution of cells in microchannels, where displacements due to cell-cell or cell-wall hydrodynamic interactions are much slower (9, 14, 16). Sedimentation in inlet reservoirs and tubings makes it difficult to control the local haematocrit, which seriously reduces the possible timescale of experiments and prevents the collection of statistically relevant data over long periods. This practical difficulty can only be partly overcome – albeit in an uncontrolled way – by stirring the suspension in the reservoirs.

Historical experiments have often considered carrying fluids of relatively high viscosity (~ 10 mPa.s) to counter this issue. They have allowed to infer information on the cell mechanical properties. However, the dynamics and lateral migration of RBCs are strongly modified in such conditions, in comparison with buffers of viscosity close to that of plasma, which is slightly above

1 mPa.s at 37°C (14, 47, 48); this makes it difficult to draw relevant conclusions about blood flow, when physiological relevance is sought.

While recent papers focused on microcirculatory dynamics still consider using viscous buffers (49), alternatives have been developed. Running experiments in microgravity conditions is one of them (14), yet it poses issues in terms of access, cost and compatibility between the allotted microgravity time and the needed experimental time. The much more accessible technique of density matching was introduced in the community in (50), then used in several studies (16, 21, 22, 25, 48, 51–55). By using iodixanol solutions, agreement between the mean density of RBCs and the carrying fluid can be reached, while the viscosity remains in an acceptable range (around 1.5 to 1.6 mPa.s at room temperature, see Section Viscosimetry)

In parallel, several other studies where the mechanical interplay between cells and flow is crucial only used the classical phosphate-buffered-saline solution as a suspending fluid, which raises the question of biases due to sedimentation (12, 56–61), in particular for those considering aggregating cells (23, 62–64). This diversity in methodology leads to question the reliability of comparisons of results obtained by different research groups working with different suspending media.

Another potential issue is that of access to blood and time between sample collection and experiments. Depending on the national legislation and on the organization of blood supply, blood samples can be studied right after collection, or a delay may be requested to perform preliminary testing of pathogens. In France, blood provided by the French Blood Bank (Etablissement Français du Sang, EFS) is generally qualified after three days but can be obtained at day 0 (D0) in a few specific centers relying on regular donors. One may also wonder, in the case of unexpected contingencies requiring to postpone (part of) an experiment: can it be pursued a few days later and still provide trustful results? And more generally, how long after collection can a blood sample be used for reliable experiments? This opens the question of the impact of blood sample storage on the mechanical properties of red blood cells and their behavior under a variety of flow conditions.

However, the determination of the geometrical and mechanical properties of RBCs (e.g. visco-elastic moduli, initial stresses in the cell at rest, etc...) is not an easy task. The outputs of a given experiment are related to these properties but the inverse problem is tricky to solve, as several of the mechanical characteristics of the RBCs are often implicated in the observed situation. Moreover, complex modeling has to be called for, which can often be resolved only through numerical simulations. As an example, the rheological properties of the membrane of an elastic capsule (a much simpler object than an RBC) has only recently been determined by solving the inverse problem of the flow of such a capsule in the center of a channel (65).

In this paper, we propose to evaluate the impact of blood conservation as well as that of density matching on physical properties of RBCs, through a set of various and complementary experiments enabling to probe various RBC behaviors under different flow conditions. Each of them has proven in the recent years to allow for a better understanding of the impact of specific control parameters (like the viscosity of the external fluid, or the flow strength) and/or of drugs that modify the cell mechanical properties on their behavior under such flow conditions. Since we aim at providing guidelines for in-vitro experiments that would mimic as much as possible the mechanical properties of RBCs freshly collected, we will restrict our study to the first week after collection. Storing blood for more than two weeks has a marked effect on red blood cell morphology and fragility (66, 67).

RBC deformability under high and steady stress (until 30 Pa) was probed by an Ektacytometry technique while dissipative mechanisms within the cell were probed in a dedicated microfluidic chip to study the Cell shape recovery after the transient deformation of RBCs. These first two experiments require to use rather viscous suspending media and have only been used to assess the impact of the conservation method, together with the following experiment. The Cell flipping dynamics under shear flow of an isolated RBC was explored in the different tested buffer solutions, thus exploring the individual mechanical properties under lower stress (around 0.2 Pa) compared to the first two experiments (at 3-30 Pa). The impact of the choice of the buffer solution was also assessed through two experiments scanning RBC collective properties: Viscosimetry and Structuration under Poiseuille flow.

For each of these experiments, a set of parameters defining the duration of initial storage in days (D0 to D7), the conservation conditions (see Sec. Storage conditions) and the buffer used for RBC suspension preparation (see Sec. Preparation of RBC suspensions) has been tested, as summarized in Fig. 1. Additional parameters have been varied to control the flow conditions in the different experiments. The range of these parameters has been carefully chosen to avoid sedimentation, when the buffer used for RBC re-suspension does not match the density of RBCs.

MATERIALS AND METHODS

Storage conditions

After blood from healthy donors was collected in 3 mL EDTA or citrate tubes, three storage protocols were tested: in collection tubes, *i.e.* in autologous plasma with EDTA or citrate, or after washing and immediate transfer of RBCs into a

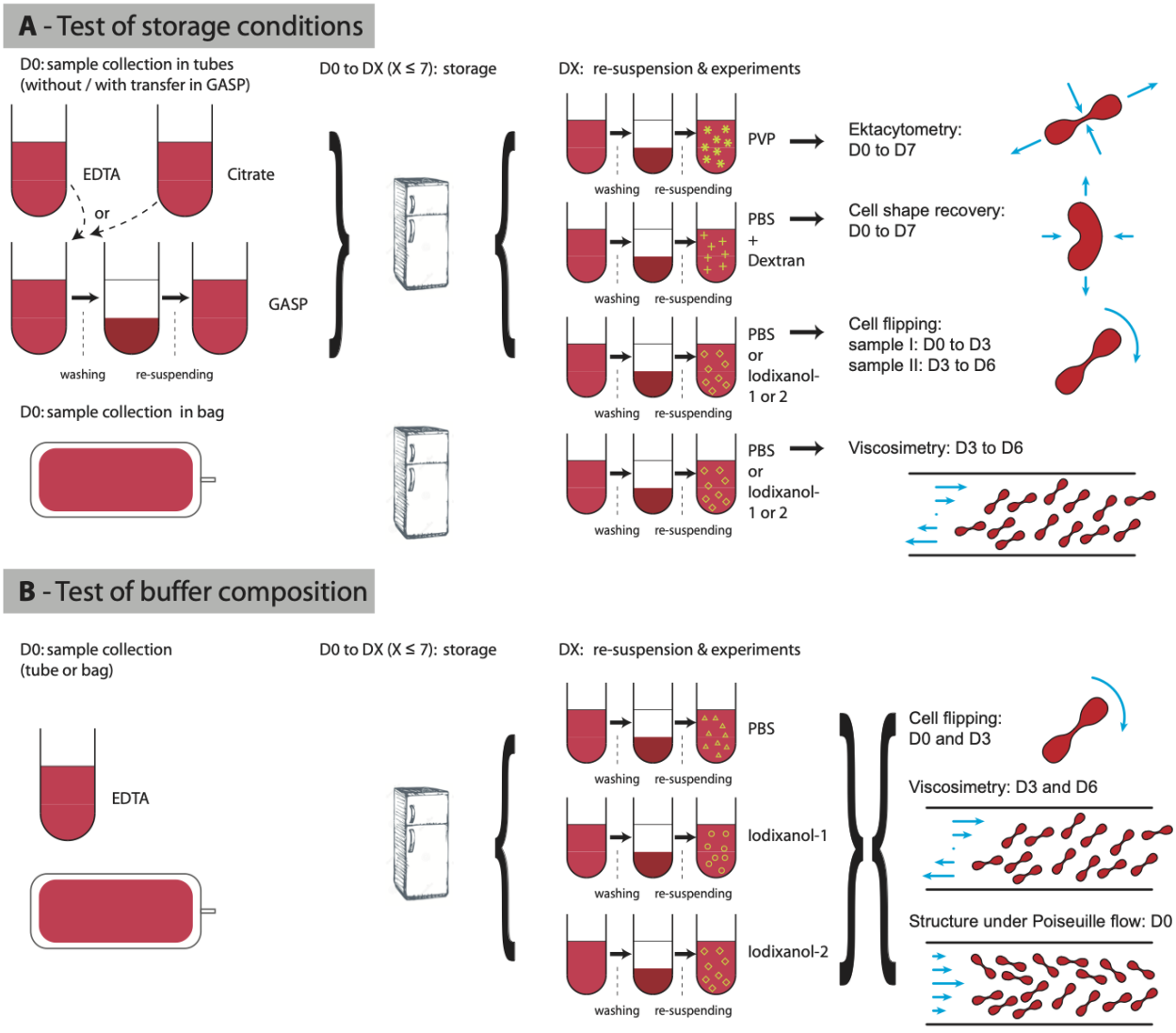

Figure 1: Summary of the protocols tested in this work and corresponding RBC deformation and interaction modes. (A) Tests of storage conditions consists in testing different conservation media (cells stored in autologous plasma with EDTA or citrate, or cells stored in GASP), except for rheology experiments, and conservation duration (see Sec. Storage conditions). They were made through four different experiments. The range of days depends on the constraints for each experimental configuration. (B) Tests of suspending medium mimicking plasma were made in three different buffer solutions (PBS, Iodixanol-1 and Iodixanol-2, see Sec. Preparation of RBC suspensions) through three different experiments. As schematized on the last column, the chosen experiments focus on different modes of deformation of RBCs, as well as on different interaction modes (isolated or concentrated cells). PBS: phosphate buffer saline; PVP: polyvinylpyrrolidone; GASP: glucose-albumin-sodium-phosphate.

Glucose-Albumin-Sodium-Phosphate (GASP) solution. GASP is a PBS solution (PBS tablet (P4417 from Sigma Aldrich, Saint-Quentin-Fallavier, France) diluted in 200 mL of deionized, ultrapure water) with 2 g/L BSA (A7906 from Sigma) and 2 g/L glucose (G8270 from Sigma).

For the GASP solution, washing was performed the same day as collection (D0) by diluting blood with a PBS solution (with a mixing ratio of 1:3). Then the suspension was centrifuged. For most experiments requiring small amounts of cells, 2 mL Eppendorf tubes were used in tabletop centrifuges (*e.g.* Heathrow Scientific Sprout, Vernon Hills, IL, USA, running at 6000 rpm). The typical operating time was 2-4 minutes at an average acceleration of 1400 g. The supernatant was withdrawn with a pipette and fresh PBS solution was added; the procedure was repeated twice. Finally, the cells were gently re-suspended in GASP with a total volume identical to the initial blood volume, so that the haematocrit was unchanged. In the following, the three storage media will be denoted as *EDTA, Citrate* and *GASP*.

For viscosimetry measurements, as larger quantities of blood were needed, a 450 mL blood bag from a healthy donor was collected (provided by EFS Auvergne-Rhône-Alpes). The bag was a standard blood-pack unit supplemented with Citrate-Phosphate-Dextrose (CPD) for preservation.

All samples were stored at 2-8°*C* until they were prepared for experiments. RBC suspensions to be used in experiments were prepared at different storage times after blood collection, from the same day (D0) up to 7 days later (D7).

Preparation of RBC suspensions

The preparation of RBC suspensions consists in separating RBCs from the storage medium before re-suspending them in different suspending buffers. Below, we first describe the two buffers used for experiments requiring high viscosities to increase significantly the hydrodynamic stress undergone by the cells, which we use to test the impact of storage conditions (type of anticoagulant and storage time) on RBC deformability. We then describe the three buffers aimed at mimicking plasma, which we mainly use to test the impact of buffer composition and in certain cases of storage conditions.

Ektacytometry experiments were run with polyvinylpyrrolidone (PVP) solutions (Mechatronics, Zwaag, The Netherlands), as in (68–70). The viscosity of PVP is 30 mPa.s at room temperature. Cell shape recovery experiments were run in PBS solutions + 90 g/L of Dextran (Dextran from Leuconostoc spp., Mw = 2,000,000, #95771 Sigma Aldrich). The viscosity of this solution has been measured to be 31 mPa.s at room temperature (71).

For Cell flipping dynamics under shear flow, Viscosimetry and Structuration under Poiseuille flow experiments, we used three suspending media:

- PBS solution (1 tablet per 200 mL water) + 2 g/L BSA (A7906 from Sigma), named *PBS* hereafter.
- PBS tablet dissolved in 200 mL of a mixture of 68.5 % water and 31.5 % Optiprep from Axis Shield (v/v) + 2 g/L BSA, named *Iodixanol-1* hereafter, as used in (16, 21, 22, 25, 48, 50–52, 55).
- 68.5% of nominal PBS solution (a PBS tablet dissolved in 200 mL of water) mixed with 31.5 % Optiprep (v/v) + 2 g/L BSA, named *Iodixanol-2* hereafter, as used in (53, 54).

The physical properties of these suspending media are summarized in Table 1. The first two suspending media (PBS and Iodixanol-1) are regularly used in the literature on human RBC dynamics at the micro-scale. Both Iodixanol-1 and Iodixanol-2 solutions provides density matching. The Iodixanol-2 has emerged as a serious alternative as it corrects the hyperosmolarity of the Iodixanol-1. Iodixanol-1 has the same salt concentration as the standard PBS solution, while in Iodixanol-2, the salt concentration is reduced by 31.5 %. Note that in the literature, different concentrations of BSA and other additives such as glucose may be used, but we restricted our study to these three media.

	PBS	Iodix.-1	Iodix.-2	Plasma
Viscosity (mPa.s)	0.98	1.58	1.57	1.4-1.6
Density (g/cm^3)	1.005	1.103	1.100	1.025
Osmolarity (mOsm/L)	290	386	298	280-300

Table 1: Properties of suspending media and plasma at 24°C. Osmolarities were measured with an osmometer using freezing point depression (Advanced Instruments Model 2020 Micro Osmometer, Norwood MA, USA), and densities by weighting 20 mL of solution, with an estimated error of 0.003. Viscosities were measured as described in the Viscosimetry section. For plasma: the viscosity at 24°C is interpolated from the normal range at 37°C (72) and measurements at 16°C in (73), density at 24°C is interpolated from (74) and osmolarity is given in (75).

After being washed three times as described in Section Storage conditions, RBCs were re-suspended in an appropriate volume of the chosen suspending medium to control the resulting haematocrit. The total duration of this procedure was less than 30 minutes. All experiments were performed right after and could last up to 3 hours.

Experimental tests

For each experiment, blood from a single donor was considered, except for the cell flipping experiment where two different samples were used, one from D0 to D3 and the other one from D3 to D6. Experiments were performed right after preparation.

Cell flipping dynamics under shear flow

In this experiment, the behavior of isolated cells under shear flow far from walls was probed. A very dilute suspension of RBCs (volume fraction ~ 0.01%) was injected in a plane-plane Couette flow chamber with a gap of 200 μm. As described in details in (48), in order to obtain information on the dynamics of all cells in the field of view and given the large thickness of the flow chamber, the suspension was monitored by a digital holographic microscope. Post-processing of images allows refocusing numerically on each cell so as to obtain its projected shape perpendicular to the shear-gradient direction. For each cell projection, the angle Ψ of its main axis with the flow direction and the aspect ratio $r_a \geq 1$ between its two main axis, were computed (see Fig. 2A). Statistics on these two parameters could then be obtained by accumulating data as the cells flow in the chamber. In (48), this procedure was used to establish the whole transition scenario for the dynamics of isolated RBCs, for shear rates γ between 0.5 and 200 s^{-1}, and viscosity of the carrying fluid equal to 1.5 or 25 mPa.s. The situation using a viscosity of 1.5 mPa.s corresponds to a viscosity close to that of plasma and a Iodixanol-1 solution was needed in order to observe statistically relevant population before cell sedimentation on the bottom plane takes place. For the sake of comparison, we focused here on a single value of the shear rate, γ = 200 s^{-1}, which was high enough to allow for good sampling of the flowing suspension before the cells are too close to the bottom plane while remaining in the physiological range. Only cells located at least 30 μm from the walls were included in the statistics. Statistical data on at least 6000 cell pictures, which were observed during sequences between 25 and 75 s, were then obtained for the two parameters Ψ and r_a. At the shear rate of 200 s^{-1}, it has been shown that cells exhibit a quasi-fixed shape which can be strongly deformed (stomatocyte-like shape) (3, 48, 76). Due to the elongational component of the flow, the angle of the main axis is centered on 0, while high aspect ratios with strong dispersion can be observed.

Cell shape recovery

The transient deformation of RBCs flowing out of a microfluidic constriction was used to evaluate the mechanical signature of cells (71, 77). The microfluidic geometry consists in a 50 μm wide microchannel implementing a series of width oscillations corresponding to 5 μm wide and 10 μm long constrictions associated with a 25 μm wide and 10 μm long enlargements (see Fig. 3A). Due to the repetition of the width oscillation, the cells were sequentially elongated along and perpendicular to the flow direction, hence ensuring a rapid centering effect as illustrated in Fig. 3A. This effect is crucial as it guarantees that all cells exit the last constriction on the same streamline, which allows for the direct comparison of their behavior. The RBC suspension was injected into the microfluidic device using a pressure driven flow controlled using a pressure regulator (MFC^{TM}-EZ Fluigent, Paris) with a precision of 1 mbar. Video-microscopic recordings of the cells' behavior were performed with an inverted phase contrast microscope (Leica DMI 4000B, Germany) with a X40 magnification and a high speed camera (Phantom Miro LAB310, USA). Thanks to the image analysis procedure described elsewhere (71), the major and minor axes of the ellipse that has the same normalized second central moments as the cell are retrieved. They are then used to calculate the deformation index D defined as $D = (a - b)/(a + b)$, where $2a$ and $2b$ are the lengths of the ellipse axes along and perpendicular to the flow direction, respectively. Diluted cell suspensions (~ 10^6 cells/μL, *i.e.* H_t=9%) were used in order to avoid the flow of multiple cells simultaneously in the wavy section of the channel. Experiments were repeated twice and a total statistics including ~ 60-80 cells per conditions were recorded.

In (71), the experimental conditions (geometry, flow speed and buffer viscosity) were varied in order to highlight two different shape recovery processes at the exit of the last geometric constriction, according to the hydrodynamic stress. Here, the applied pressure at the inlet was set to 200 mBar, which corresponds to typical cell velocities of the order of 7 mm/s and 1 mm/s in the wavy and larger sections respectively, when using 90 g/L dextran in PBS buffer. In such conditions, stretching of the cells was observed as they exit the last constriction before recovering a steady shape in the larger part of the channel as illustrated in Fig. 3. The amplitude of deformation in the wavy section of the channel (calculated over the 4 last oscillations to avoid being impacted by the entry position of the cell), ΔD, along with the minimum of the elongation index, D_{out}, - which corresponds to the maximum cell elongation normal to the flow direction due to the increase in channel width - were extracted as presented in Fig. 3B. The time necessary for the cell to recover a stationary

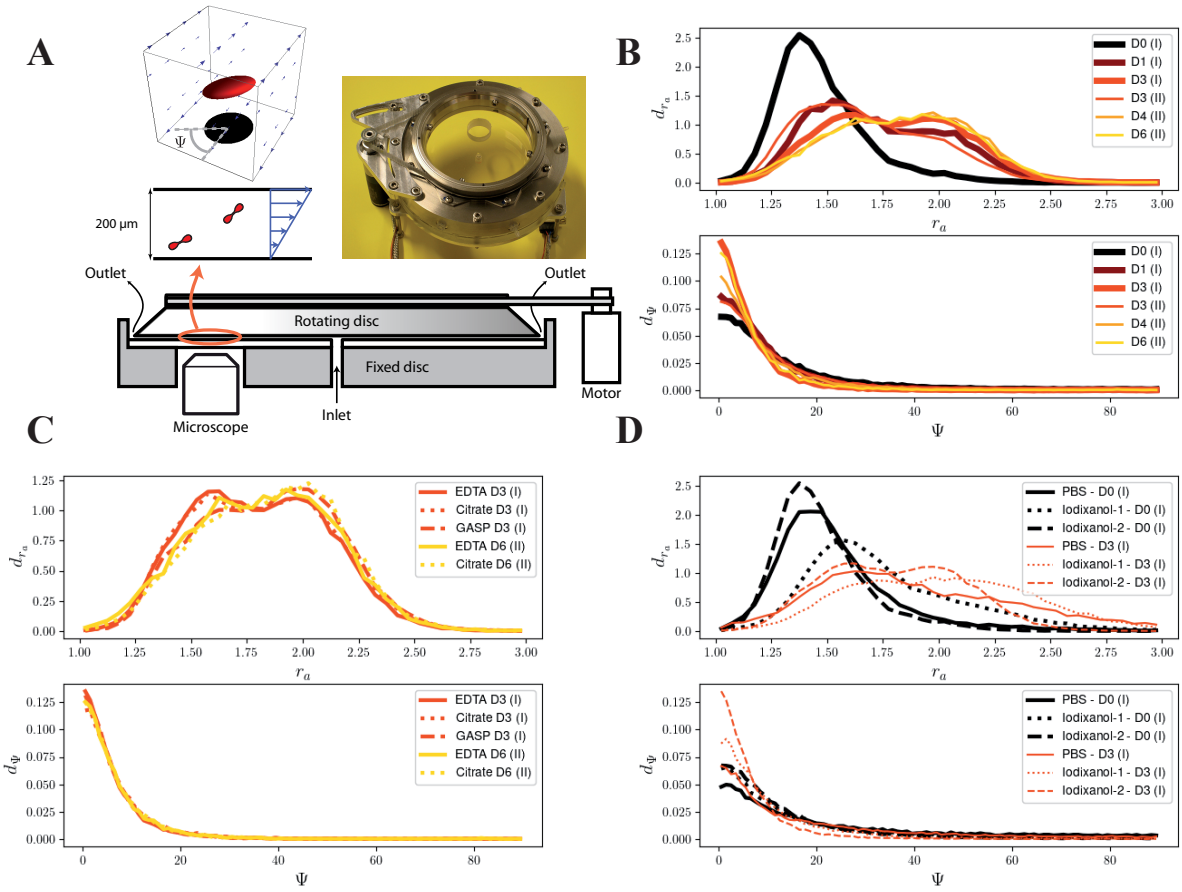

Figure 2: Cell flipping experiment. (A) Sketch of the experimental set-up. Cells trapped in the gap between the two plates are observed. The projection of each cell along the shear direction is determined, and characterized by its aspect ratio r_a and angle of the long axis relatively to flow direction Ψ. (B) Effect of aging, for cells conserved in EDTA. Suspending solution is Iodixanol-2. Donor I from D0 to D3, donor II from D3 to D6. Top: density distribution d_{r_a} of apparent aspect ratio r_a. Bottom: density distribution d_Ψ of the projected angle Ψ (in °). (C) Effect of conservation medium in cell flipping experiment, for two different days: D3 for donor I, D6 for donor II. Suspending solution is Iodixanol-2. Top: density distribution d_{r_a} of apparent aspect ratio r_a. Bottom: density distribution d_Ψ of projected angle Ψ. (D) Effect of suspending medium in cell flipping experiment, for two different days with donor I (D0 and D3, conserved in EDTA). Top: density distribution d_{r_a} of apparent aspect ratio r_a. Bottom: density distribution d_Ψ of projected angle Ψ.

shape, noted hereafter τ_r, was calculated by fitting the end of the curve D versus the time t (from D_{out} until end of the curve) by an exponential growth function of the type $D = C_1 + C_2 \times \exp(\frac{C_3 - t}{\tau_r})$, where C_1, C_2 and C_3 are constant to be adjusted. The representation of $1/\tau_r$ versus D_{out} has been previously used to differentiate cells with different mechanical signatures due to pharmaceutical treatments (lysophosphatidylcholine and diamide) at different concentrations and diseases (77). On the contrary, ΔD was found to be only sensitive to large deformability changes associated with high drug concentrations.

Ektacytometry

RBC deformability was also assessed at 37°C at shear stresses of 3 and 30 Pa by laser diffraction analysis (ektacytometry), using the Laser-assisted optical rotational cell analyzer (LoRRca MaxSis, RR Mechatronics, Hoorn, The Netherlands). The system has been described elsewhere in detail (68). Briefly, 7 μL of stored RBC suspension was mixed with 1 mL PVP solution and sheared into the Couette system. A laser went through the sheared suspension and a camera recorded the diffraction pattern. The computer fitted an outline to the elliptic diffraction pattern which allowed the estimation of the length and width of the fitted ellipse. Then, an elongation index (EI) was calculated as follows: (length-width)/(length+width). An increase in the EI indicates greater RBC deformability.

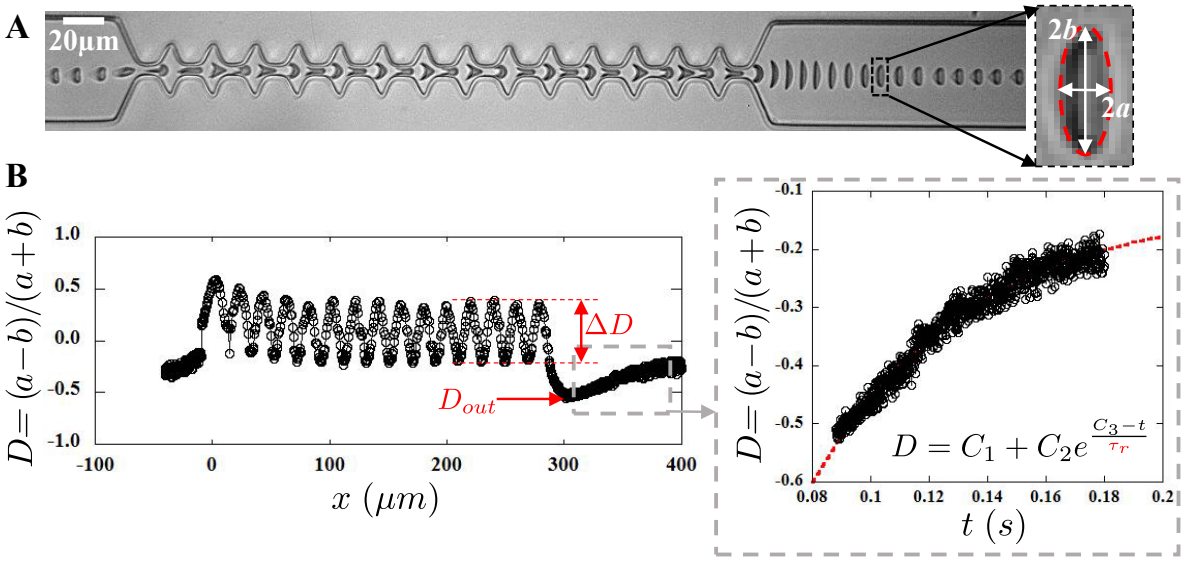

Figure 3: Principle of the cell shape recovery approach. (A) Sequence of deformation of a RBC flowing through the microfluidic wavy geometry. The close-up illustrates the adjustment of the cell contour by an ellipse and the determination of $2a$ and $2b$ the axes of the ellipse along and perpendicular to the flow direction respectively. (B) Corresponding evolution of the deformation index D versus the cell position x. The entry of the first constriction has been arbitrarily selected as the origin of the position. The inset shows the shape recovery process as a function of time. The parameters of interest are the amplitude of deformation ΔD, measured over the 4 last width oscillations, the maximum elongation at the exit D_{out} and the shape recovery time τ_r, which are reported in Fig. 5.

Viscosimetry

The bulk effective viscosity η of RBC suspensions was measured at imposed shear rate in a rheometer. As these experiments require larger sample volumes, the RBC washing protocol was adapted: 15 mL tubes were filled with 5 mL blood and 10 mL PBS and centrifuged at an average acceleration of 720 g for 5 minutes. After the third centrifugation and supernatant removal, RBCs were placed in two 50 mL tubes and centrifuged again in order to obtain an homogeneous pellet of cells, whose concentration is close to 100% thanks to cell deformability (78).

This pellet of cells was used to prepare RBC suspensions with the same three suspending media as used in section Cell flipping dynamics under shear flow. For each medium, suspensions of decreasing cell concentrations (from 48 to 0% in volume) were prepared by dilution. Volume fractions in the studied suspensions were estimated by centrifugation of glass capillaries filled with the suspensions. For the two isodense suspending medium, the suspensions were diluted once with a PBS solution so that centrifugation could be effective.

Before the suspensions were placed in the rheometer, they were kept under continuous gentle agitation on a roller mixer, then kept vertical during 2 minutes to allow the potentially present air bubbles to reach the surface. 5 mL of each suspension were prepared, of which 3.8 mL were taken to be placed in the rheometer. We used an Anton Paar MCR 301 rheometer (Graz, Austria) with a double gap Couette geometry (SN21094). The axial length of the effective measuring gap was 40 mm while the gaps had a thickness of 0.415 and 0.464 mm. Measurements were run at 24°C. The device was cleaned and dried between each experiment. In order to reduce the influence of cell sedimentation that could bias the results, we decided to work at only one shear rate. We chose 400 s^{-1}, a good compromise to obtain high enough stress for accurate sensitivity without any inertial effect and within the range of shear rates of in-vivo circulation. The measurement was made right after the suspension was gently poured in the rheometer cup with a micropipette. We checked that several successive measurements with PBS as a suspending medium, with the same suspension being left in the rheometer, yielded similar results, insuring thus that our procedure allows for an unbiased measurement even with PBS, when sedimentation is possible. Indeed, from the filling to the end of the measurement, we estimated the elapsed time to be around 60s, thus allowing only for a cell migration of order 100 microns, to be compared with the measuring height of 40 mm.

We also checked the relevance of comparing different measurements while the whole geometry is dismounted and cleaned between each of them as follows. Measuring two times the same initial suspension (prepared then with a double volume of 10 mL) with a full dismounting/washing/drying of the geometry between the two measurements, lead to variations in the measured

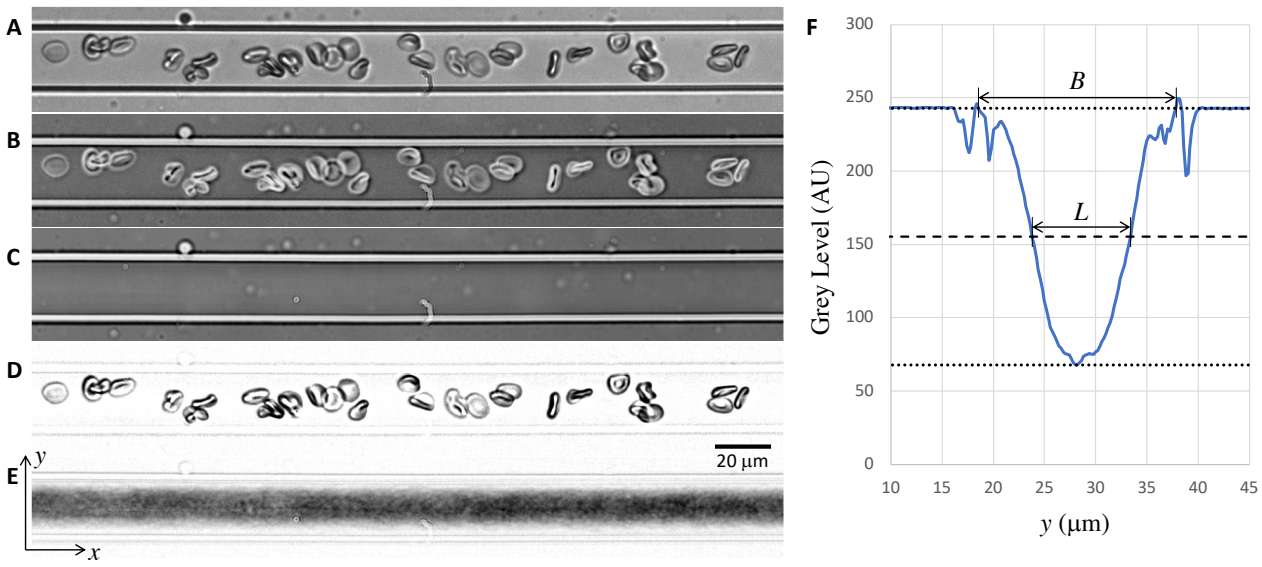

Figure 4: RBC structuration under Poiseuille flow and associated metrics. (A) Representative snapshot from an experiment with Iodixanol-1 used as a suspending medium and H_t = 2.2%, ΔP = 50 mbar, yielding V_{max} = 3.4 mm/s; (B) Negative of the image in panel A; (C) Negative background obtained as the median of 100 negative images (1/20 in the sequence, including image in panel B); (D) Image in panel C subtracted from image in panel B to remove background; (E) Mean intensity of all negative snapshots with background removed (1/20 in the sequence, including image in panel D). (F) Mean grey level profile obtained by averaging D along the channel length. An estimate of the width of the RBC enriched central area is given by B, which is defined as the central interval for which grey levels in the profile are below the background level. An estimate of the adimensional CFL thickness is deduced as $\delta = (W - B)/(2W)$, where W is the channel width. L represents the full width at half maximum.

viscosity of order 0.5 %. Filling procedure can also induce variations (by creating bubbles, retaining part of the liquid, etc..). Filling with 3.7 or 3.9 mL of suspension instead of 3.8 mL lead to less than 1% variation in the measured viscosity.

The suspending medium viscosities at 24°C are η_0 = 0.98, 1.58 and 1. 57 mPa.s for the PBS, Iodixanol-1 and Iodixanol-2 respectively. For estimating the contribution of red blood cells to the viscosity, we therefore considered the relative viscosity of a given suspension η/η_0.

Structuration under Poiseuille flow

A cell-free layer (CFL) can build up near the vessel walls in small vessels, due to hydrodynamic interactions between RBCs and the walls (79). The CFL presence is obvious for moderate confinements (vessels with diameters of 10 μm or more) and small haematocrits (25), and its thickness decreases when increasing the local haematocrit or confinement. Below, we present the experimental configuration used for studying the structuration of RBCs under Poiseuille flow, using long (~ 1 cm) PDMS-glass microfluidic channels with square cross-sections (20 μm ×20 μm).

The protocol used for the fabrication of single PDMS-glass microchannels has been described in detail elsewhere (25). Before use, microchannels were incubated overnight with a PBS solution containing 2.5 mg/mL BSA (Eurobio, Les Ulis, France) in order to prevent RBC adhesion onto microchannel walls. The microchannel was then placed on the stage of a Leica DMRXA2 microscope, glass cover slip facing a ×20 (NA = 0.4) long-working distance objective. RBC suspensions with controlled feed haematocrit H_{feed} in the range 1 to 10% were flown by imposing a pressure drop ΔP between the microchannel inlet and outlet in the range of 45 to 110 mbar using a pressure controller (MicroFluidics Control System 8C, Fluigent). The generated flow rate was sufficiently high to prevent RBC sedimentation, even when PBS was used as a suspending medium. Image sequences of the flow were recorded using an external collimated light source (Leica EL6000) and a high-speed camera (pco.dimax S). Typical image sequences were composed of ≃ 10000 16 bit snapshots, acquired at a frequency of 1200 fps. Fig. 4A displays one of these snapshots after conversion to 8 bits. These image sequences were used to introduce metrics characterizing the RBC structuration under Poiseuille flow and to determine the mean tube haematocrit and maximal velocity of RBCs, as follows.

We recently presented a quantitative method to determine the haematocrit profile in a microchannel with a square cross

section (25). However, this method requires linear extrapolation of optical density profiles in the vicinity of the channel walls. Here, we introduce a simpler and faster method - based on two metrics characterizing the RBC structuration - sufficient to make comparisons between different experimental situations. For that purpose, we first kept one out of twenty snapshots in the image sequence. This ensures that, for any pressure drop, each RBC contributes only once to the measurement. These snapshots were inverted (Fig. 4B) and a median image over the 100 first images was computed, yielding the negative background image (Fig. 4C). This background image was subtracted from all the inverted images, yielding dark RBCs highly visible on a light background (Fig. 4D). A mean image was computed from this stack (Fig. 4E). Finally, a gray value profile over the channel width was deduced by averaged along the channel length (Fig. 4F). This profile was used to get an estimate of the adimensional CFL thickness as $\delta = (W - B)/(2W)$, where B is an estimate of the width of the RBC enriched central area, see Fig. 4 and W is the channel width. Because of the uncertainty induced by intensity fluctuations in the vicinity of channel walls, an additional metric, the full width at half maximum L, was also extracted from this profile.

As the RBC suspensions were sufficiently diluted, the local tube haematocrit H_t could be determined by counting, following (22), with the following modifications: the RBCs were counted in 100 images evenly sampled throughout the sequence to deduce their average number. The average haematocrit was deduced by multiplying this number by the ratio of the average volume of a single RBC (90 μm^3, see (80)) over the volume of the channel. Finally, the maximal RBC velocity V_{max} was estimated by tracking 5 RBCs approximately located at the channel center, using image pairs such as RBCs have moved a distance approximately equal to the channel thickness. The measurement was performed at 4 time points equally sampled over the total duration of the image sequence. The maximal RBC velocity was estimated as the maximal value of all these measurements.

A total of 46 experiments was performed, with H_t between 0.2 and 3.6% and V_{max} between 0.5 and 36 mm/s. We have checked that there were no correlation between velocities and haematocrits in these experiments.

RESULTS AND DISCUSSION

Effect of storage conditions

Flipping cells

Figs. 2B and 2C show the effects of aging and storage conditions for cells resuspended in Iodixanol-2. The conclusions are similar for the two other suspending media (data not shown).

As seen in Fig. 2B, whether from D0 to D3 or from D3 to D6, storing several days the RBCs has a moderate effect on their apparent aspect ratio and on their angle relative to flow direction, showing that the main dynamical features are preserved. We observe an increase in the apparent aspect ratio, in particular a shift in the position of the first peak (located at around 1.4 at D0), by an amount of up to 10% after three days. In the meantime, the proportion of RBCs aligned with the flow ($\Psi \simeq 0$) increases as the RBCs get older. From the modeling carried out in (48), the shift in apparent aspect ratio can be simply interpreted by a shift in the aspect ratio at rest, that is, of the ratio between the short axis and the long axis of the RBCs. By analogy with the experiments lead in the hyper-osmotic Iodixanol-1, on which we comment later on, we may interpret the increase in aspect ratio as a consequence of a loss of cell volume, which is agreement with other observations at longer times (81). Other causes such as alterations of RBC mechanical properties should however not be disregarded.

These aging effects are also observed in the two other conservation media; in particular, the marked evolution between D0 and D1 is the same whatever the choice of conservation medium (see supplemental material). Indeed, as seen in Fig. 2C, the choice of conservation medium has little effect on the dynamics, though cells conserved in GASP seem to have increased slightly more their aspect ratio after 3 days, that is, to have lost more volume.

Cell shape recovery

Fig. 5 presents the evolution of the amplitude of deformation ΔD, the maximum elongation at the exit D_{out}, and the shape recovery time τ according to storage time, for the 3 different storage media.

In order to look at the effect of the conservation buffer on the RBCs response, we first compare the different readouts at D0 for the 3 media. We assume that the greater deformability of RBCs corresponded to their physiological state and that any modifications due to time or to the storage medium would be associated with a loss of deformability. We can see in Fig. 5, a slight decrease in amplitude of deformation (up to 14%), as well as an overall increase in shape recovery time of RBCs stored in Citrate and GASP compared to those stored in EDTA (~71 and 27% respectively). This indicates that EDTA should be preferred when working on the day of the blood collection.

For RBCs stored in EDTA, a small drop of deformability is observed after D0, highlighted by both a decrease in ΔD and in D_{out}, and an increase in time necessary for RBCs to recover a steady shape after exiting the last geometric restriction. The following days, deformability seems to stabilize, although τ shows a slight tendency to increase gradually up to D7. RBCs

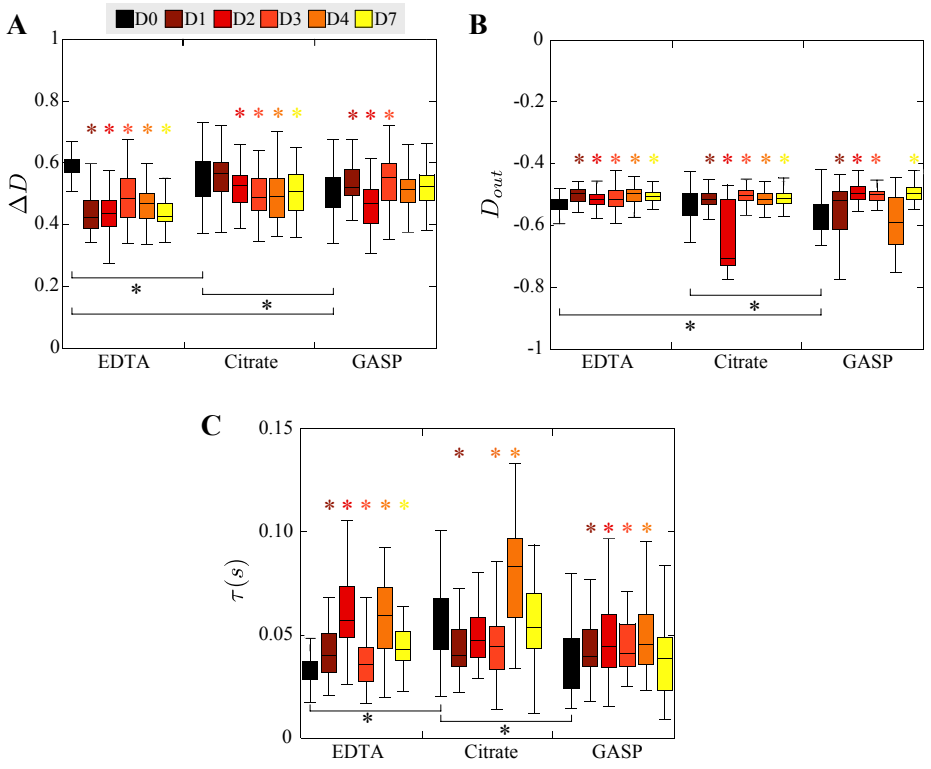

Figure 5: Cell shape recovery experiment. Evolution of the amplitude of deformation (A), the maximum elongation at the exit (B) and the shape recovery time of the RBCs (C) versus time, according to the three different conservation solutions. Data are represented in terms of median; the top and bottom of the box mark the upper quartile (UQ) and lower quartile (LQ) respectively. The error bars mark the minimum and maximum values within the data set that fall within $[UQ + 1.5(UQ - LQ); LQ - 1.5(UQ - LQ)]$. Black * indicate the significant differences ($p < 0.05$) between the different conservation solutions at D0, calculated by Kruskall-Wallis's test, with Dunn's post hoc analysis. Colored * indicate the significant differences ($p < 0.05$) between D0 and DX ($1 \leq X \leq 7$), calculated by Kruskall-Wallis's test, with Dunn's post hoc analysis.

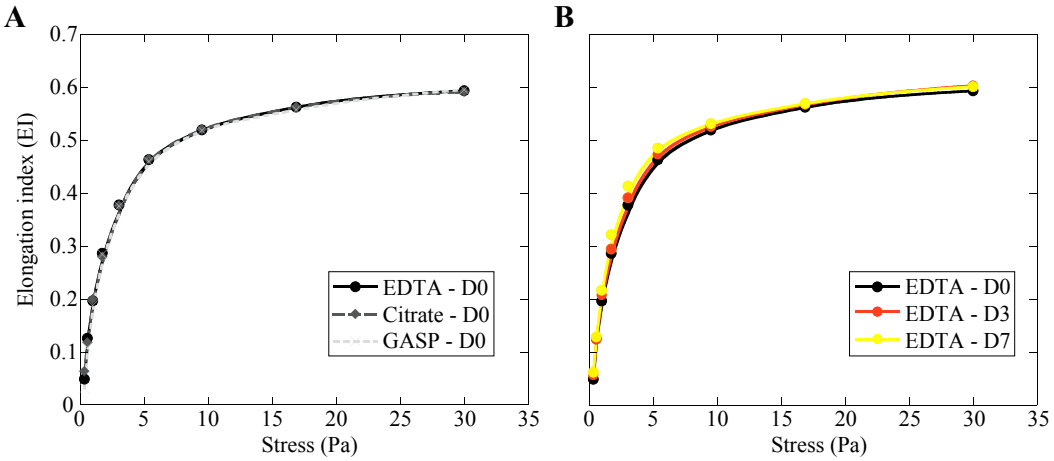

Figure 6: Ektacytometry experiment. (A) Elongation index for three different conservation solutions at day D0. (B) Elongation index for the EDTA conservation solution at days D0, D3 and D7.

stored in Citrate and GASP present a deformability that seems to be more stable in the short term (D0 to D2) and then slightly decreased. Therefore, if one needs to use blood samples several successive days, Citrate and GASP should be preferred.

From previous experiments (77) performed on chemically treated RBCs, it appears that τ and in a lesser extend D_{out}, are strongly impacted by diamide treatment - a molecule reported to induce the formation of disulfide bonds between spectrin proteins and thus increase RBCs shear modulus (42, 82). On the other hand the reduction of the surface to volume ratio of the RBC membrane, induced by the loss of RBC membrane through vesiculation associated with lysolecithin treatment (83), tends to affect both D_{out} and τ. Here, the fact that both D_{out} and τ are modified upon storage time, supports the idea that a loss of volume due to aging of the cells would be responsible for the change in deformability. This corroborates the observations made in the Cell flipping dynamics under shear flow experiments.

Ektacytometry

Fig. 6A shows no effect of the conservation solution used on RBC deformability determined by ektacytometry at D0. Moreover, storage for 7 consecutive days in EDTA was not accompanied by large changes in RBC deformability (Fig. 6B). These results are in line with a previous similar study led in (84).

Viscosimetry

Viscosity measurements were run only at D3 and D6. They are consistent with known viscosity values in large vessels. As shown in Fig. 7, no noticeable difference can be seen between these two days. It should be noted that, according to the other experiments, most aging effects occur between D0 and D3, a configuration not tested here.

Effect of buffer composition

Flipping cells

Fig. 2D summarizes our findings regarding the choice of the suspending medium. It appears clearly that, while the overall dynamics is unchanged, choosing Iodixanol-1 as a suspending medium leads to more elongated and deflated cells on average, which we relate to the hyper-osmoticity of the solution. This effect is quite strong at D0, while at D3, when cells have already lost some volume due to aging, the difference is less pronounced. By contrast, at D0, the behavior of cells in Iodixanol-2 is unchanged when compared to PBS solution, as could be hoped from the agreement between both solution osmolarities. The low salt concentration of Iodixanol-2 seems to have no measurable impact on the cell flipping.

Viscosimetry

Fig. 7 shows that for all suspending media, a reasonable agreement with the empirical model proposed in (85) by Pries et al. (and widely used since then) is obtained, considering that inter-individual variability prevents from hoping better agreement.

Up to haematocrits of 30 %, no noticeable variation of the relative bulk viscosity with the nature of the suspending medium has been observed. For higher haematocrits though, underestimations of around 10% are found with the isodense solutions, and are surprisingly more pronounced for Iodixanol-2, in contrast with other experiments that tend to show more similarities in RBC behavior in PBS and Iodixanol-2. However, Iodixanol solutions have a viscosity that is about 50% higher than PBS solutions. Vitkova et al. (86) have shown that the intrinsic viscosity of RBC suspensions exhibits a minimum when varying the viscosity of the suspending medium, due to variations of RBC dynamics in shear flow. This could be responsible for the slightly lower relative viscosities measured in isodense solutions. On the other hand, the higher osmolarity of Iodixanol-1 leads to more deflated cells (as also shown in the cell flipping experiments), which partly compensates for the previous effect.

Structuration under Poiseuille flow

Fig. 8 displays the estimate of the CFL thickness δ and the full width at half maximum of the mean grey level profile L, both normalized by the channel width, as a function of local tube haematocrit, for the three suspending media. For the considered channel width (20 μm), we never clearly observed single file RBC flow, yielding values of δ which are always smaller than that estimated for a single file of width equal to the largest dimension of a single RBC (δ would be ~ 0.3, for a RBC diameter of $\sim 8\mu$m). For all media, increasing the RBC volume fraction induces a decrease of the CFL thickness, with a concomitant increase of the width of the enriched RBC central region, as expected from the general understanding of RBC structuration in the microcirculation (87–89), both in vivo and in vitro. Noteworthy, our results provide the first direct experimental measurements of the CFL thickness for a large range of haematocrits in 20μm side channels. Our results thus provide a reference for the validation of a large number of numerical methods recently developed for the simulation of collective RBC behavior. Besides,

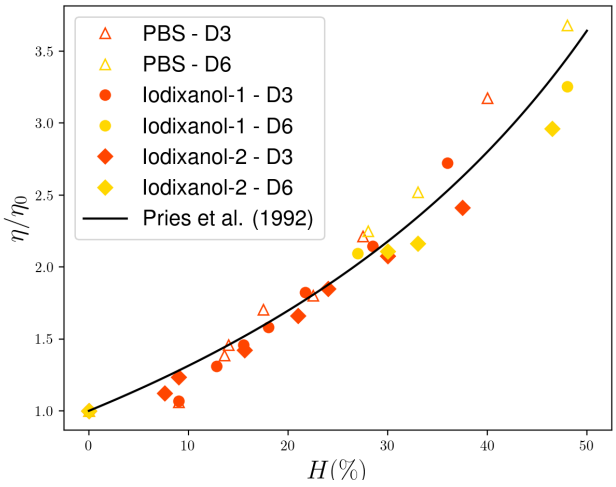

Figure 7: Relative viscosity η/η_0, where η_0 is the viscosity of the suspending fluid, as a function of haematocrit. Blood comes from a blood bag where it was conserved either 3 or 6 days. Three suspending media are considered: △: PBS; •: Iodixanol-1; ◆: Iodixanol-2. The full line corresponds to the asymptotic value for large tube diameters of the blood viscosity model given by Pries et al. (85).

they demonstrate the minor impact of the suspending medium, the influence of which cannot be identified within experimental noise.

CONCLUSION

Our set of complementary experiments characterizing the mechanical behavior of red blood cells under different flow configurations allow to draw the following conclusions:

1. Conservation medium. We showed that the choice of conservation medium between EDTA, Citrate, or laboratory-made GASP has little impact on the mechanical response of RBCs under shear, either under high (ektacytometry) or low (cell flipping experiment) stress. In a more complex geometry which allows to explore not only the elastic response but also the viscous one (cell shape recovery experiment), we highlighted a better stability at short time when cells were stored in Citrate and GASP.

2. Storage time. While cells under high stress present a stable response in time, the picture is different in low stress experiments, where a clear aging effect between D0 and D3 has been noted, though the overall dynamics is preserved. Stability seems to be reached between D3 and D6, as also seen on viscosity curves. Since this low stress configuration corresponds more to physiological conditions in terms of buffer viscosity and flow shear rate, this means that running experiments at D0 must be preferred when possible. Similar conclusion is reached from cell shape recovery experiments, that explore complex visco-elastic response of the cells. It would be interesting in the future to assess the impact of these D0 to D1 evolutions on the rheological response of blood.

3. Buffer composition. Our study on individual behavior of RBCs through the cell flipping experiment reveals that choosing Iodixanol-2 as a density matching solution is a good pick. By contrast, the hyper-osmotic Iodixanol-1 solution leads to modification of the aspect ratio of the cells. The difference between this suspending medium and PBS becomes smaller at D3, when aging effects take place, showing that aging or hyper-osmolarity have a similar effect, yet non cumulative. Finally, this impact of choosing Iodixanol-1 as a buffer solution seemingly disappears when collective effects are considered, as clearly highlighted in the Poiseuille flow experiments. Our conclusion is that the results from previous studies from the literature run with Iodixanol-1 are still valid in view of describing physiologically relevant situations, though the bias on individual dynamics should be kept in mind, as for Refs. (16, 48). For experiments run in the future, we recommend using Iodixanol-2 as a buffer solution.

   One should keep in mind however that density matching of all RBCs in a given batch cannot be reached since the density of RBCs increases as they get older, before they are eliminated in the spleen. The range of densities is typically 1.06-1.13 g. mL^{-1} (81, 90, 91). Density variations in the population of cells are associated with biochemical (91) and mechanical

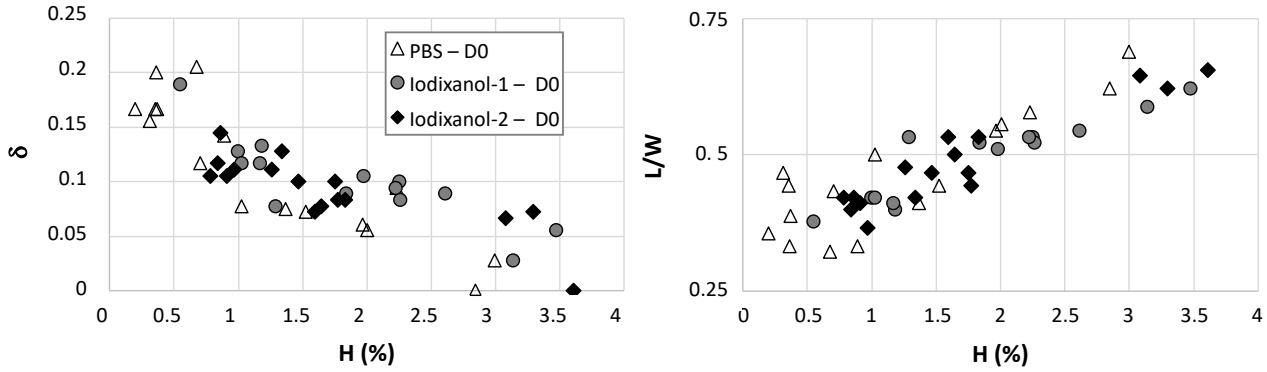

Figure 8: Effect of suspending solution and tube haematocrit on RBC structuration under Poiseuille flow at D0. Left: Estimate of adimensional CFL thickness; Right: Half width of the distribution (L) normalized by channel size (W=20μm). Symbols: △: PBS; •: Iodixanol-1; ◆: Iodixanol-2.

changes such as: volume, aspect ratio, visco-elastic modulus, etc. (81, 92), also affecting their mechanical response like shear-induced lift (16).

Our study enriches the existing consensus on other aspects related to in-vitro experimentation with RBCs, such as the use of glutaraldehyde for stiffening them (93), or as protocols for blood collection and preparation for analysis (68, 84, 94). These latter studies include the withdrawal protocol, the choice of anticoagulant (EDTA is proposed rather than heparin in (68)), or the washing protocol (which was followed in the present study). Note that in (68), it is advised not to store samples more than a few hours. While this prescription can be followed in routine analysis, the unavoidable contingencies of research made it relevant to explore this point further. For clinical applications involving blood transfusion, the relevant time scale for checking the effect of conservation conditions of RBCs is instead of a few weeks. It has already been thoroughly explored in the literature, e. g. in (95, 96). Conclusions are that while a substantial amount of RBCs get strongly impaired after a few weeks, adequate washing may help in recovering at least partly their ability to perfuse the vascular network.

Beyond the above conclusions, the present study also provides a comprehensive set of results for RBCs behavior under very different flow configurations, which, all together, have been chosen to probe many of the possible RBC deformation and interaction modes, as illustrated in Fig. 1. In a context where 3D numerical simulations of a large number of RBCs are now widespread, our study provides a robust benchmark for validating the codes, which is sometimes only done through quasi-static configurations like stretching by optical tweezers: this has been shown in Ref. (97) not to be sufficient. Benchmark studies based on experiments under flow need to be further developed, keeping in mind that, as demonstrated in Ref. (98), "this is in fact not always sufficient as the robustness of the numerical results to physical/numerical parameters may be so large that a good agreement may be reached by chance".

The work that was carried out here may be extended in the future to more complex configurations, in view of reaching higher physiological relevance. First, aggregation between cells is an important phenomenon, that can only be discarded in high shear rate situations, when flow stress overcomes adhesion forces. Being larger, aggregates of cells will sediment even faster than isolated cells, which may require the use of density-matching solutions. However, the complexity of aggregation processes makes it uncertain the impact of adding another molecule such as iodixanol to the buffer.

Second, more complex in-vitro studies mimicking more closely in-vivo environments by considering e.g. channels covered with endothelial cells (99) require to take into account the co-existence of several types of cells and finding compromises for the suspending medium, whose influence on each cell type has ideally to be estimated.

AUTHOR CONTRIBUTIONS

AM, SL, PC, MF, SL, EN, TP, CR, GC and EF participated in the early stages of method sharing and designed the research. AM, SL, FY, MF, CM, EN, TP, CR, GC and EF ran experiments and treated their data. AM, PC, MF, SL, EN, TP, CR, GC and EF analysed the data and wrote the article. GC and EF coordinated the work.

DECLARATION OF INTEREST

The authors declare no competing interests.

ACKNOWLEDGMENTS

This collaborative work was made possible by CNRS GDR 3570 MECABIO. We wish to gratefully acknowledge François Caton, Sébastien Cazin, Paul Duru, Emmanuèle Helfer, Alexandra Lamouliatte, Mickaël Marin, Frédéric Risso, Anne-Virginie Salsac, and Annie Viallat for useful discussions. The collaboration and experiment on cell flipping was developed in the framework of microgravity experiments supported by CNES (VP145) and hosted in Novespace facilities while the shear flow chamber was developed by the Swedish Space Corporation for earlier ESA sponsored microgravity experiments (MASER 11). Poiseuille flow experiments were supported by the European Research Council under ERC Consolidator grant agreements 615102 (BrainMicroFlow) and 772191 (MultiphysMicroCaps).

REFERENCES

1. Ku, D. N., 1997. Blood flow in arteries. Ann. Rev. Fluid Mech. 29:399–434.
2. Chien, S., 1970. Shear Dependence of Effective Cell Volume as a Determinant of Blood Viscosity. Science 168:977–979.
3. Mauer, J., S. Mendez, L. Lanotte, F. Nicoud, M. Abkarian, G. Gompper, and D. A. Fedosov, 2018. Flow-Induced Transitions of Red Blood Cell Shapes under Shear. Phys. Rev. Lett. 121:118103.
4. Thurston, G. B., 1973. Frequency and shear rate dependence of viscoelasticity of human blood. Biorheology 10:375–381.
5. Poiseuille, J.-M., 1835. Recherches sur les causes du mouvement du sang dans les vaisseaux capillaires. Comptes rendus hebdomadaires des séances de l'Académie des sciences 1:554–560.
6. Fåhræus, R., and T. Lindqvist, 1931. The viscosity of the blood in narrow capillary tubes. Am. J. Physiol. 96:562–568.
7. Fåhræus, R., 1929. The suspension stability of the blood. Physiol. Rev. 9:241–274.
8. Popel, A. S., and P. C. Johnson, 2005. Microcirculation and hemorheology. Annu. Rev. Fluid Mech. 37:43–69.
9. Goldsmith, H. L., 1971. Red cell motions and wall interactions in tube flow. Fed. Proc. 30:1578.
10. Yamaguchi, S., T. Yamakawa, and H. Niimi, 1992. Cell-free plasma layer in cerebral microvessels. Biorheology 29:251–260.
11. Fedosov, D. A., B. Caswell, A. S. Popel, and G. E. Karniadakis, 2010. Blood Flow and Cell-Free Layer in Microvessels. Microcirculation 17:615–628.
12. Sherwood, J. M., J. Dusting, E. Kaliviotis, and S. Balabani, 2012. The effect of red blood cell aggregation on velocity and cell-depleted layer characteristics of blood in a bifurcating microchannel. Biomicrofluidics 6:024119.
13. Narsimhan, V., H. Zhao, and E. S. G. Shaqfeh, 2013. Coarse-grained theory to predict the concentration distribution of red blood cells in wall-bounded Couette flow at zero Reynolds number. Phys. Fluids 25:061901.
14. Grandchamp, X., G. Coupier, A. Srivastav, C. Minetti, and T. Podgorski, 2013. Lift and Down-Gradient Shear-Induced Diffusion in Red Blood Cell Suspensions. Phys. Rev. Lett. 110:108101.
15. D.Katanov, G. Gompper, and D. A. Fedosov, 2015. Microvascular blood flow resistance: Role of red blood cell migration and dispersion. Microvasc. Res. 99:57 – 66.
16. Losserand, S., G. Coupier, and T. Podgorski, 2019. Migration velocity of red blood cells in microchannels. Microvasc. Res. 124:30.
17. Fenton, B. M., R. T. Carr, and G. R. Cokelet, 1985. Non-uniform red cell distribution in 20 to 100 μm bifurcations. Microvasc. Res. 29:103 – 126.
18. Pries, A. R., K. Ley, M. Claassen, and P. Gaethgens, 1989. Red cell distribution at microvascular bifurcations. Microvasc. Res. 38:81–101.

19. Barber, J. O., J. P. Alberding, J. M. Restrepo, and T. W. Secomb, 2008. Simulated two-dimensional red blood cell motion, deformation, and partitioning in microvessel bifurcations. Ann. Biomech. Eng. 36:1690–1698.

20. Doyeux, V., T. Podgorski, S. Peponas, M. Ismail, and G. Coupier, 2011. Spheres in the vicinity of a bifurcation: elucidating the Zweifach–Fung effect. Journal of Fluid Mechanics 674:359–388.

21. Shen, Z., G. Coupier, B. Kaoui, B. Polack, J. Harting, C. Misbah, and T. Podgorski, 2016. Inversion of hematocrit partition at microfluidic bifurcations. Microvasc. Res. 105:40 – 46.

22. Roman, S., A. Merlo, P. Duru, F. Risso, and S. Lorthois, 2016. Going beyond 20 μm-sized channels for studying red blood cell phase separation in microfluidic bifurcations. Biomicrofluidics 10:034103.

23. Kaliviotis, E., J. Sherwood, and S. Balabani, 2017. Partitioning of red blood cell aggregates in bifurcating microscale flows. Scientific reports 7:44563.

24. Balogh, P., and P. Bagchi, 2018. Analysis of red blood cell partitioning at bifurcations in simulated microvascular networks. Phys. Fluids 30:051902.

25. Merlo, A., M. Berg, P. Duru, F. Risso, Y. Davit, and S. Lorthois, 2022. A few upstream bifurcations drive the spatial distribution of red blood cells in model microfluidic networks. Soft Matter 18:1463–1478.

26. Picart, C., J.-M. Piau, H. Gaillard, and P. Carpentier, 1998. Human blood shear yield stress and its hematocrit dependence. J. Rheol. 42:1–12.

27. Neu, B., and H. Meiselman, 2002. Depletion-mediated red blood cell aggregation in polymer solutions. Biophys. J. 83:2482–2490.

28. Bagchi, P., P. Johnson, and A. Popel, 2005. Computational fluid dynamic simulation of aggregation of deformable cells in a shear flow. Biochem. Eng. J. 127:1070–1080.

29. Pereverzev, Y., O. V. Prezhdo, M. Forero, E. Sokurenko, and W. Thomas, 2005. The Two-Pathway Model for the Catch-Slip Transition in Biological Adhesion. Biophys. J. 89:1446–1454.

30. Ziherl, P., and S. Svetina, 2007. Flat and sigmoidally curved contact zones in vesicle–vesicle adhesion. Proc. Natl. Acad. Sci. USA 104:761–765.

31. Flormann, O., D.and Aouane, L. Kaestner, C. Ruloff, C. Misbah, T. Podgorski, and C. Wagner, 2017. The buckling instability of aggregating red blood cells. Sci. Rep. 7:7928.

32. Hoore, M., F. Yaya, T. Podgorski, C. Wagner, G. Gompper, and D. A. Fedosov, 2018. Effect of spectrin network elasticity on the shapes of erythrocyte doublets. Soft Matter 14:6278–6289.

33. Baskurt, O. K., A. Temiz, and H. J. Meiselman, 1998. Effect of superoxide anions on red blood cell rheologic properties. Free Radic. Biol. Med. 24:102–110.

34. Hierso, R., X. Waltz, P. Mora, M. Romana, N. Lemonne, P. Connes, and M. D. Hardy-Dessources, 2014. Effects of oxidative stress on red blood cell rheology in sickle cell patients. Brit. J. Haematol. 166:601–606.

35. Tomaiuolo, G., 2014. Biomechanical properties of red blood cells in health and disease towards microfluidics. Biomicrofluidics 8:051501.

36. Park, Y., C. A. Best, A. T., N. S. Gov, S. A. Safran, G. Popescu, S. Suresh, and M. S. Feld, 2010. Metabolic remodeling of the human red blood cell membrane. Proc. Natl. Acad. Sci. USA 107:1289–1294.

37. Fermo, E., D. Monedero-Alonso, P. Petkova-Kirova, A. Makhro, L. Pérès, G. Bouyer, A. P. Marcello, F. Longo, G. Graziadei, W. Barcellini, A. Bogdanova, S. Egee, L. Kaestner, and P. Bianchi, 2020. Gardos channelopathy: functional analysis of a novel KCNN4 variant. Blood Adv. 4:6336–6341.

38. Mansour-Hendili, L., S. Egée, D. Monedero-Alonso, G. Bouyer, B. Godeau, B. Badaoui, A. Lunati, C. Noizat, A. Aissat, L. Kiger, C. Mekki, V. Picard, S. Moutereau, P. Fanen, P. Bartolucci, L. Garçon, F. Galactéros, and B. Funalot, 2021. Multiple thrombosis in a patient with Gardos channelopathy and a new KCNN4 mutation. Am. J. Hematol. 96:E318–E321.

39. Pérès, L., D. Monedero Alonso, M. Nudel, M. Figeac, J. Bruge, S. Sebda, V. Picard, W. El Nemer, C. Preudhomme, C. Rose, S. Egée, and G. Bouyer, 2021. Characterisation of Asp669Tyr Piezo1 cation channel activity in red blood cells: an unexpected phenotype. Brit. J. Haematol. 194:e51–e55.

40. Da Costa, L., J. Galimand, O. Fenneteau, and N. Mohandas, 2013. Hereditary spherocytosis, elliptocytosis, and other red cell membrane disorders. Blood Rev. 27:167–178.

41. Goldsmith, H. L., and J. Marlow, 1972. Flow Behaviour of Erythrocytes. I. Rotation and Deformation in Dilute Suspensions. Proc. R. Soc. B 182:351.

42. Fischer, T. M., M. Stöhr-Liesen, and H. Schmidt-Schönbein, 1978. The red cell as a fluid droplet: tank tread-like motion of the human erythrocyte membrane in shear flow. Science 202:894.

43. Goldsmith, H. L., and J. C. Marlow, 1979. Flow Behaviour of Erythrocytes. II. Particle motions in concentrated suspensions of ghost cells. J. Colloid Interface Sci. 71:383–407.

44. Fischer, T. M., H. C. W., M. Stöhr-Liesen, H. Schmid-Schönbein, and R. Skalak, 1981. The stress-free shape of the red blood cell membrane. Biophys. J. 34:409–22.

45. Bitbol, M., 1986. Red blood cell orientation in orbit $C = 0$. Biophys. J. 49:1055.

46. Matsunaga, D., Y. Imai, C. Wagner, and T. Ishikawa, 2016. Reorientation of a single red blood cell during sedimentation. J. Fluid Mech. 806:102–128.

47. Fischer, T., and R. Korzeniewski, 2013. Threshold shear stress for the transition between tumbling and tank-treading of red blood cells in shear flow: dependence on the viscosity of the suspending medium. J. Fluid Mech. 736:351.

48. Minetti, C., V. Audemar, T.Podgorski, and G. Coupier, 2019. Dynamics of a large population of red blood cells under shear flow. J. Fluid Mech. 864:408.

49. Zhou, Q., J. Fidalgo, M. O. Bernabeu, M. S. N. Oliveira, and T. Krüger, 2021. Emergent cell-free layer asymmetry and biased haematocrit partition in a biomimetic vascular network of successive bifurcations. Soft Matt. 17:3619–3633.

50. Roman, S., S. Lorthois, P. Duru, and F. Risso, 2012. Velocimetry of red blood cells in microvessels by the dual-slit method: Effect of velocity gradients. Microvasc. Res. 84:249.

51. Mantegazza, A., M. Ungari, F. Clavica, and D. Obrist, 2020. Local vs. Global Blood Flow Modulation in Artificial Microvascular Networks: Effects on Red Blood Cell Distribution and Partitioning. Frontiers in Physiology 11:1117.

52. Mantegazza, A., F. Clavica, and D. Obrist, 2020. In vitro investigations of red blood cell phase separation in a complex microchannel network. Biomicrofluidics 14:014101.

53. de Monchy, R., J. Rouyer, F. Destrempes, B. Chayer, G. Cloutier, and E. Franceschini, 2018. Estimation of polydispersity in aggregating red blood cells by quantitative ultrasound backscatter analysis. J. Acoust. Soc. Am. 143:2207–2216.

54. Fenech, M., V. Girod, V. Claverìa, S. Meance, M. Abkarian, and B. Charlot, 2019. Microfluidic blood vasculature replicas using backside lithography. Lab Chip 19:2096–2106.

55. Audemar, V., T. Podgorski, and G. Coupier, 2022. Rheology and structure of a suspension of deformable particles in plane Poiseuille flow. Phys. Fluids 34:042013.

56. Sneha Maria, M., B. S. Kumar, T. S. Chandra, and A. K. Sen, 2015. Development of a microfluidic device for cell concentration and blood cell-plasma separation. Biomedical Microdevices 17:115.

57. Robinson, M., H. Marks, T. Hinsdale, K. Maitland, and G. Coté, 2017. Rapid isolation of blood plasma using a cascaded inertial microfluidic device. Biomicrofluidics 11:024109.

58. Passos, A., J. M. Sherwood, E. Kaliviotis, R. Agrawal, C. Pavesio, and S. Balabani, 2019. The effect of deformability on the microscale flow behavior of red blood cell suspensions. Physics of Fluids 31:091903.

59. Saadat, A., D. A. Huyke, D. I. Oyarzun, P. V. Escobar, I. H. Øvreeide, E. S. G. Shaqfeh, and J. G. Santiago, 2020. A system for the high-throughput measurement of the shear modulus distribution of human red blood cells. Lab Chip 20:2927–2936.

60. Pskowski, A., P. Bagchi, and J. D. Zahn, 2021. Investigation of red blood cell partitioning in an in vitro microvascular bifurcation. Artificial Organs 45:1083–1096.

61. Recktenwald, S. M., K. Graessel, F. M. Maurer, T. John, S. Gekle, and C. Wagner, 2022. Red blood cell shape transitions and dynamics in time-dependent capillary flows. Biophys. J. 121:23–36.

62. Brust, M., O. Aouane, M. Thiébaud, D. Flormann, C. Verdier, L. Kaestner, M. Laschke, H. Selmi, A. Benyoussef, T. Podgorski, G. Coupier, C. Misbah, and C. Wagner, 2014. The plasma protein fibrinogen stabilizes clusters of red blood cells in microcapillary flows. Sci. Rep. 4:4348.

63. Sherwood, J. M., D. Holmes, E. Kaliviotis, and S. Balabani, 2014. Spatial Distributions of Red Blood Cells Significantly Alter Local Haemodynamics. Plos One 9:1–13.

64. Claverìa, V., O. Aouane, M. Thiébaud, M. Abkarian, G. Coupier, C. Misbah, T. John, and C. Wagner, 2016. Cluster of red blood cells in microcapillary flow: hydrodynamic versus macromolecule induced interaction. Soft Matter 12:8235–8245.

65. Wang, X.-Y., A. Merlo, C. Dupont, A.-V. Salsac, and D. Barthès-Biesel, 2021. A microfluidic methodology to identify the mechanical properties of capsules: comparison with a microrheometric approach. Flow 1:E8.

66. Roussel, C., M. Dussiot, M. Marin, A. Morel, P. A. Ndour, J. Duez, C. Le Van Kim, O. Hermine, Y. Colin, P. A. Buffet, and P. Amireault, 2017. Spherocytic shift of red blood cells during storage provides a quantitative whole cell–based marker of the storage lesion. Transfusion 57:1007–1018.

67. Gautam, R., J.-Y. Oh, M. B. Marques, R. A. Dluhy, and R. P. Patel, 2018. Characterization of Storage-Induced Red Blood Cell Hemolysis Using Raman Spectroscopy. Laboratory Medicine 49:298–310.

68. Baskurt, O. K., M. Boynard, G. C. Cokelet, P. Connes, B. M. Cooke, S. Forconi, F. Liao, M. R. Hardeman, F. Jung, H. J. Meiselman, G. Nash, N. Nemeth, B. Neu, B. Sandhagen, S. Shin, G. Thurston, and J.-L. Wautier, 2009. New guidelines for hemorheological laboratory techniques. Clin. Hemorheol. Microcirc. 42:75–97.

69. Renoux, C., M. Romana, P. Joly, S. Ferdinand, C. Faes, N. Lemonne, S. Skinner, N. Garnier, M. Etienne-Julan, Y. Bertrand, M. Petras, G. Cannas, L. Divialle-Doumdo, E. Nader, D. Cuzzubbo, Y. Lamarre, A. Gauthier, X. Waltz, K. Kebaili, C. Martin, A. Hot, M. D. Hardy-Dessources, V. Pialoux, and P. Connes, 2016. Effect of Age on Blood Rheology in Sickle Cell Anaemia and Sickle Cell Haemoglobin C Disease: A Cross-Sectional Study. PLoS One 11:e0158182.

70. Nemkov, T., S. C. Skinner, E. Nader, D. Stefanoni, M. Robert, F. Cendali, E. Stauffer, A. Cibiel, C. Boisson, P. Connes, and A. D'Alessandro, 2021. Acute Cycling Exercise Induces Changes in Red Blood Cell Deformability and Membrane Lipid Remodeling. Int. J. Mol. Sci. 22:896.

71. Amirouche, A., J. Esteves, A. Lavoignat, S. Picot, R. Ferrigno, and M. Faivre, 2020. Dual shape recovery of Red Blood Cells flowing out of a microfluidic constriction. Biomicrofluidics 14:024116.

72. Kesmarky, G., P. Kenyeres, M. Rabai, and K. Toth, 2008. Plasma viscosity: A forgotten variable. Clinical Hemorheology and Microcirculation 39:243–246.

73. Malomuzh, N. P., L. A. Bulavin, V. Y. Gotsulskyi, and A. A. Guslisty, 2020. Characteristic changes in the density and shear viscosity of human blood plasma with varying protein concentration. Ukrainian Journal of Physics 65:151–156.

74. Trudnowski, R. J., and R. C. Rico, 1974. Specific Gravity of Blood and Plasma at 4 and 37°C. Clinical Chemistry 20:615–616.

75. Gennari, F. J., 1984. Serum Osmolality - Uses And Limitations. New England Journal Of Medicine 310:102–105.

76. Lanotte, L., J. Mauer, S. Mendez, D. A. Fedosov, J.-M. Fromental, V. Claverìa, F. Nicoud, G. Gompper, and M. Abkarian, 2016. Red cells dynamic morphologies govern blood shear thinning under microcirculatory flow conditions. Proc. Nat. Acad. Sci. 113:13289–13294.

77. Faivre, M., C. Renoux, A. Bessaa, L. D. Costa, P. Joly, A. Gauthier, and P. Connes, 2020. Mechanical signature of Red Blood Cells flowing out of a microfluidic constriction is impacted by membrane elasticity, cell surface-to-volume ratio and diseases. Frontiers in Physiology 11:576.

78. Chaplin, H. J., and P. L. Mollison, 1952. Correction for Plasma Trapped in the Red Cell Column of the Hematocrit. Blood 7:1227–1238.

79. Secomb, T. W., 2017. Blood flow in the microcirculation. Annual Review of Fluid Mechanics 49:443–461.

80. Baskurt, O. K., R. A. Farley, and H. J. Meiselman, 1997. Erythrocyte aggregation tendency and cellular properties in horse, human, and rat: a comparative study. American Journal of Physiology-Heart and Circulatory Physiology 273:H2604–H2612.

81. Linderkamp, O., E. Friederichs, T. Boehler, and A. Ludwig, 1993. Age dependency of red blood cell deformability and density: studies in transient erythroblastopenia of childhood. British J. Haematology 83:125–129.

82. Safeukui, I., P. A. Buffet, G. Deplaine, S. Perrot, V. Brousse, A. Ndour, M. Nguyen, O. Mercereau-Puijalon, P. H. David, G. Milon, and N. Mohandas, 2012. Quantitative assessment of sensing and sequestration of spherocytic erythrocytes by the human spleen. Blood 120:424–430.

83. Clark, M., N. Mohandas, and S. Shohet, 1983. Osmotic gradient ektacytometry: comprehensive characterization of red cell volume and surface maintenance. Blood 61:899–910.

84. Makhro, A., R. Huisjes, L. P. Verhagen, M. Mañú-Pereira, E. Llaudet-Planas, P. Petkova-Kirova, J. Wang, H. Eichler, A. Bogdanova, R. van Wijk, J. L. Vives-Corrons, and L. Kaestner, 2016. Red Cell Properties after Different Modes of Blood Transportation. Frontiers in physiology 7:288.

85. Pries, A. R., D. Neuhaus, and P. Gaehtgens, 1992. Blood viscosity in tube flow: dependence on diameter and hematocrit. Am. J. Physiol. 263:H1770–H1778.

86. Vitkova, V., M.-A. Mader, B. Polack, C. Misbah, and T. Podgorski, 2008. Micro-Macro Link in Rheology of Erythrocyte and Vesicle Suspensions. Biophys. J. 95:33.

87. Pries, A. R., T. W. Secomb, and P. Gaehtgens, 1996. Biophysical aspects of blood flow in the microvasculature. Cardiovascular research 32:654–667.

88. Maeda, N., Y. Suzuki, J. Tanaka, and N. Tateishi, 1996. Erythrocyte flow and elasticity of microvessels evaluated by marginal cell-free layer and flow resistance. Am. J. Phys. 271:H2454–H2461.

89. Lorthois, S., 2019. Blood suspension in a network. In A. Viallat, and M. Abkarian, editors, Dynamics of Blood Cell Suspensions in Microflows, CRC Press, Boca Raton, 257–286. 1st edition.

90. Leif, R. C., and J. Vinograd, 1964. The distribution of buoyant density of human erythrocytes in bovine albumin solutions. PNAS 51:520–528.

91. Cohen, N. S., J. E. Ekholm, M. G. Luthra, and D. J. Hanahan, 1976. Biochemical characterization of density-separated human erythrocytes. Biochimica Biophysica Acta 419:229–242.

92. Linderkamp, O., and H. J. Meiselman, 1982. Geometric, Osmotic, and Membrane Mechanical Properties of Density-Separated Human Red Cells. Blood 59:1121–1127.

93. Abay, A., G. Simionato, R. Chachanidze, A. Bogdanova, L. Hertz, P. Bianchi, E. van den Akker, M. von Lindern, M. Leonetti, G. Minetti, C. Wagner, and L. Kaestner, 2019. Glutaraldehyde - A Subtle Tool in the Investigation of Healthy and Pathologic Red Blood Cells. Frontiers Physiol. 10.

94. Bull, B., S. Chien, J. Dormandy, H. Kiesewetter, S. Lewis, G. Lowe, H. Meiselman, S. Shohet, J. Stoltz, J. Stuart, and P. Teitel, 1986. Guidelines for measurement of blood viscosity and erythrocyte deformability. Clin. Hemorheol. 6:439–453.

95. Yoshida, T., and S. S. Shevkoplyas, 2010. Anaerobic storage of red blood cells. Blood Transfus. 8:220–36.

96. Reinhart, W. H., N. Z. Piety, J. W. Deuel, A. Makhro, T. Schulzki, N. Bogdanov, J. S. Goede, A. Bogdanova, R. Abidi, and S. S. Shevkoplyas, 2015. Washing stored red blood cells in an albumin solution improves their morphologic and hemorheologic properties. Transfusion 55:1872–1881.

97. Sigüenza, J., S. Mendez, and F. Nicoud, 2017. How should the optical tweezers experiment be used to characterize the red blood cell membrane mechanics? Biomech. Model. Mechanobiol. 16:1645–1657.

98. Nicoud, F., V. Zmijanovic, and S. Mendez, 2019. Reaching a good agreement between computational hemodynamics results and in-vitro data is not enough. Comp. Meth. Biomech. Biomed. Eng. 22:S78–S79.

99. Tsvirkun, D., A. Grichine, A. Duperray, C. Misbah, and L. Bureau, 2017. Microvasculature on a chip: study of the Endothelial Surface Layer and the flow structure of Red Blood Cells. Sci. Rep. 7:45036.